J Solid State Electrochem (2008) 12:323–327
DOI 10.1007/s10008-007-0394-1

ORIGINAL PAPER

# Synthesis and electrochemical properties of $LiNi_{0.85-x}Co_xMn_{0.15}O_2$ as cathode materials for lithium-ion batteries

**Daocong Li · Chaoqun Yuan · Jiaqing Dong · Zhenghe Peng · Yunhong Zhou**

Received: 13 February 2007 / Revised: 15 July 2007 / Accepted: 16 July 2007 / Published online: 11 August 2007


**Abstract** $LiNi_{0.85-x}Co_xMn_{0.15}O_2$ cathode material was prepared by a rheological phase reaction method with $LiNO_3$, $M(NO_3)_2\ 6H_2O$ (M = Ni, Co, Mn), and citric acid as starting materials. The mixture of reactants and a proper amount of water reacted to form a rheological precursor. The rheological precursor was pretreated in autoclaves and then calcined at 750 °C under flowing oxygen. All the samples have a typical layered structure with space group *R3-m* and good electrochemical performances. The cobalt content has a significant effect on the electrochemical performance for the materials. $LiNi_{0.65}Co_{0.20}Mn_{0.15}O_2$ exhibits the best electrochemical properties in the five compounds. It gives an initial discharge capacity of 173.6mAhg$^{-1}$ (50mA g$^{-1}$, 3.0−4.3V), and the capacity rention after 50 cycles is 90.6%. This method is simple and effective for preparing cathode materials for lithium-ion batteries.

**Keywords** Lithium-ion batteries · Rheological phase reaction method · Cathode materials · Lithium nickel cobalt manganese oxides · Electrochemical properties

## Introduction

Lithium cobalt oxide ($LiCoO_2$) had been used as a cathode material of commercial lithium-ion batteries because of its excellent electrochemical properties, such as high output voltage, long life cycle, and easy preparation [1, 2]. However, the high cost and toxicity of cobalt lead to researching for other better materials. Furthermore, its capacity was restricted to a half of theoretical capacity when it is charged above 4.2V (vs $Li/Li^+$) because of structural degradation [3]. Lithium nickel oxide ($LiNiO_2$), in spite of its high capacity and low cost and toxicity, was hard to prepare and showed instability of structure and thermodynamic properties during the charge–discharge process [4–6]. $LiNi_{1-x}Co_xO_2$, which combined the advantages of $LiCoO_2$ and $LiNiO_2$, exhibited high initial discharge capacity and good cycling [7–9]. Nevertheless, the problem of safety caused by overcharge was still unsolved [10, 11].

Lithium nickel cobalt manganese oxides have attracted extensive attention, such as $LiNi_{1/3}Co_{1/3}Mn_{1/3}O_2$ [12–14] and $LiNi_{1-x-y}Co_xMn_yO_2$ [15–18]. These materials exhibit excellent properties, for example, higher capability, low cost, and safety. Therefore, lithium nickel cobalt manganese oxides are considered as one of the promising candidates to replace $LiCoO_2$ for lithium-ion batteries. In this paper, we adopt a rheological phase reaction method to synthesize $LiNi_{0.85-x}Co_xMn_{0.15}O_2$ ($x$ = 0.05, 0.10, 0.15, 0.20, 0.25) compounds with $LiNO_3$, $M(NO_3)_2\ 6H_2O$ (M = Ni, Co, Mn) and citric acid as starting materials. It is a simple and effective route for preparing electrode materials [19–22].

## Experimental

$LiNi_{0.85-x}Co_xMn_{0.15}O_2$ ($x$ = 0.05, 0.10, 0.15, 0.20, 0.25) was prepared from $LiNO_3$, $M(NO_3)_2\ 6H_2O$ (M = Ni, Co, Mn), and citric acid. $LiNO_3$ was added 5% excessively compensating for loss, which occurred in the solid-state reaction at high temperature [23]. The acid-to-metal ion

D. Li · C. Yuan · J. Dong · Z. Peng (✉) · Y. Zhou
Department of Chemistry, Wuhan University,
Wuhan 430072, People's Republic of China
e-mail: zhhpeng@126.com

ratio was 1:1. The starting materials were mixed uniformly. Then, a proper amount of deionized water was added to get a liquid–solid rheological system, and the mixture was displaced to an autoclave and heated at 80 °C for 2 h. Through the rheological phase treatment, reactants are homogeneously mixed at an atomic scale, which is beneficial to the diffusion process and reaction process. After dried and ground, the mixed powders were preheated at 600 °C for 2h and then calcined at 750 °C for 10h in flowing oxygen.

Thermal decomposition behavior of the mixed precursor was examined by thermogravimetric and differential thermal analysis (TG/DTA, Netzsch STA 449C) in static air at a heating rate of 5 °C $min^{-1}$. The crystalline structure of the prepared powder was investigated by means of powder X-ray diffraction (XRD, Shimadzu, XRD-6000) using Cu Kα radiation ($\lambda$ = 1.54056Å). Lattice parameters and unit-cell volumes were calculated by a least-squares method with the FullProf_Suite program. The powder morphology was observed by a scanning electron microscope (SEM, Hitachi, X-650).

The electrochemical cycling performance of the material was studied by assembling model test cells. Test cathode electrodes were prepared by mixing 80:15:5 (mass ratio) of active material, acetylene black, and polytetrafluoroethylene binder, respectively, in isopropyl alcohol. After rolling the mixture to be a membrane, a circular disc of 0.8cm in diameter from the membrane was cut out and pressed onto a stainless steel mesh to become a current collector and then dried at 120 °C in a vacuum furnace for 12h. The model test cells were assembled using lithium foil as an anode and 1M $LiClO_4$ in 1:1 (volume ratio) ethylene carbonate and dimethyl carbonate as an electrolyte and Celgard 2300 membrane as the separator in an argon-filled glove box. The charge–discharge cycles were carried out at room temperature with a constant current density of 50mA $g^{-1}$ and a cutoff voltage of 3.0 to 4.3V. The thermal stability of the $LiNi_{0.65}Co_{0.20}Mn_{0.15}O_2$ electrode was examined by means of DSC with a Netzsch STA 449C thermal analysis system at a heating rate of 5 °C $min^{-1}$.

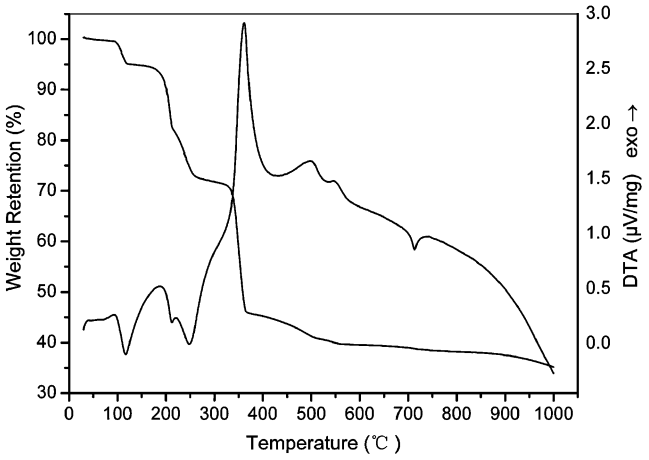


**Fig. 1** TG/DTA curves for the precursor

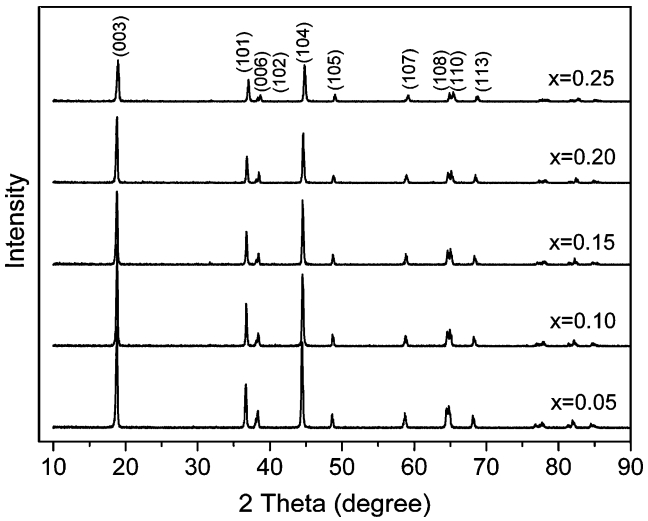


**Fig. 2** XRD patterns of $LiNi_{0.85-x}Co_xMn_{0.15}O_2$ cathode materials

## Results and discussion

The TG/DTA curves for the mixed precursor are shown in Fig. 1. The weight loss (about 6%) between room temperature to 150 °C is attributed to the removal of remnant water. The weight loss (about 24%) between 150 and 330 °C is attributed to the decomposition of nitrates and citric acid, which corresponds to endothermic peaks in the DTA curve. The weight loss (about 25%) between 330 and 370 °C is due to the decomposition and combustion of citric acid, which results in the largest exothermic peak at 361 °C in the DTA curve. The weight loss (about 6%) between 370 and 550 °C is mainly attributed to the decomposition of $Li_2CO_3$ and the formation of the layered compound. Above 550 °C, there is no major weight loss, and the layered crystallization becomes more complete.

The XRD patterns of the $LiNi_{0.85-x}Co_xMn_{0.15}O_2$ are shown in Fig. 2. All the diffraction peaks are sharp and well defined and can be indexed based on the layered α-$NaFeO_2$ (space group *R3-m*) structure. With Co content increasing, diffraction peaks move to a higher angle and the splitting of (006, 102) and (108, 110) become more obvious, which indicates that Co doping can shrink the space between layers and increase the distortion degree of the oxygen sublattice along the *c* direction [24].

Table 1 gives the lattice parameters, unit-cell volume, *c*/*a* ratio, and $I_{003}/I_{104}$ ratio of $LiNi_{0.85-x}Co_xMn_{0.15}O_2$. The lattice parameters *a* and *c* and unit-cell volume decrease continuously with increasing *x* value. The ionic radius of $Co^{3+}$ (0.053nm) is smaller than that of $Ni^{3+}$ (0.056nm), which is responsible for the reduction in lattice parameters

**Table 1** Lattice parameters, unit-cell volume, *c*/*a* ratio, and $I_{003}/I_{104}$ intensity ratio of $LiNi_{0.85-x}Co_xMn_{0.15}O_2$

| *x* value | *a* (nm) | *c* (nm) | Unit-cell volume ($nm^3$) | *c*/*a* ratio | $I_{003}/I_{104}$ |
|---|---|---|---|---|---|
| 0.05 | 0.2878 | 1.4196 | 0.1018 | 4.93 | 0.96 |
| 0.10 | 0.2872 | 1.4180 | 0.1013 | 4.94 | 1.09 |
| 0.15 | 0.2868 | 1.4169 | 0.1009 | 4.94 | 1.08 |
| 0.20 | 0.2862 | 1.4160 | 0.1004 | 4.95 | 1.16 |
| 0.25 | 0.2858 | 1.4149 | 0.1001 | 4.95 | 0.98 |

[25]. Unit-cell volume was an important parameter to measure the integrality of layered structure [26]. The sample with more layered characteristics will have a lower unit-cell volume. The *c*/*a* ratios increase slowly with Co content increasing, and the *c*/*a* values of the five samples are all above 4.899, which is the *c*/*a* ratio of the ideal close cubic packing. The ratio of $I_{003}/I_{104}$ is sensitive to the cation distribution in lattice [27,28]. The theoretical ratio depends on composition, thermal factors, valences, and other factors. The sample with Co content at 0.20 has the higher value for the $I_{003}/I_{104}$ ratio.

SEM photographs of $LiNi_{0.65}Co_{0.20}Mn_{0.15}O_2$ at different magnifications are given in Fig. 3. The primary particles size is around 0.3μm in diameter, and these small particles aggregate with each other to form a spherical secondary particle. The intercalation process of the $Li^+$ ion between the layers of the cathode is a diffusion process. Therefore, the smaller particles, which would lead to a short path for $Li^+$ ions, were favorable to intercalation, and the sample was expected to deliver a good electrochemical performance.

The charge–discharge curves of the first cycle for $LiNi_{0.85-x}Co_xMn_{0.15}O_2$ in the range 3.0–4.3V are shown in Fig. 4. The potential drop at the beginning of discharge decreases when increasing the Co content. The potential

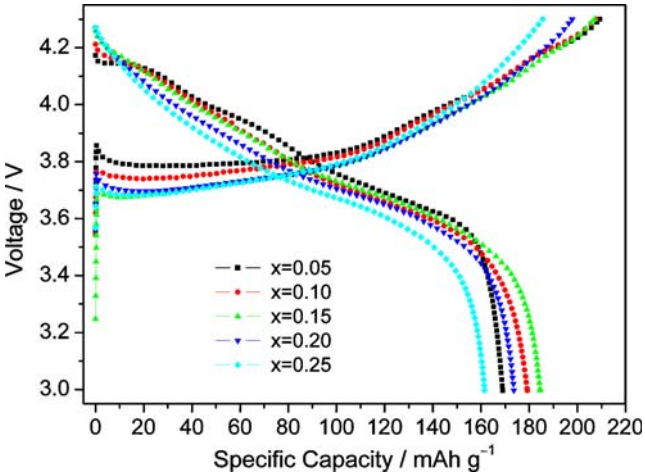


**Fig. 4** Charge–discharge curves of the first cycle for $LiNi_{0.85-x}Co_xMn_{0.15}O_2$ in the voltage range 3.0–4.3 V

drop is dominated by the resistance of electronic conduction at the beginning of discharge, indicating that increasing the Co content can improve the electronic conductivity of the synthesized materials [29]. With the *x* value increasing, initial charge–discharge curves become more smooth, which indicates that less phase transition occurs during the intercalation of $Li^+$. Every sample has comparatively high reversible capacity. When the content of Co increases, the initial charge capacity decreases, and the discharge capacity initially increases and then decreases. The sample with Co content at 0.15 has the highest initial discharge capacity of 184.5mAh $g^{-1}$.

The cycling performance for $LiNi_{0.85-x}Co_xMn_{0.15}O_2$ up to 50 cycles is shown in Fig. 5. It is found that the cathode materials synthesized by our method have excellent cyclic performance. The capacity retentions are still high after 50 cycles. When increasing the Co content, the cyclic performance becomes better, which is in correspondence with the XRD results. Moderate Co can adjust to the

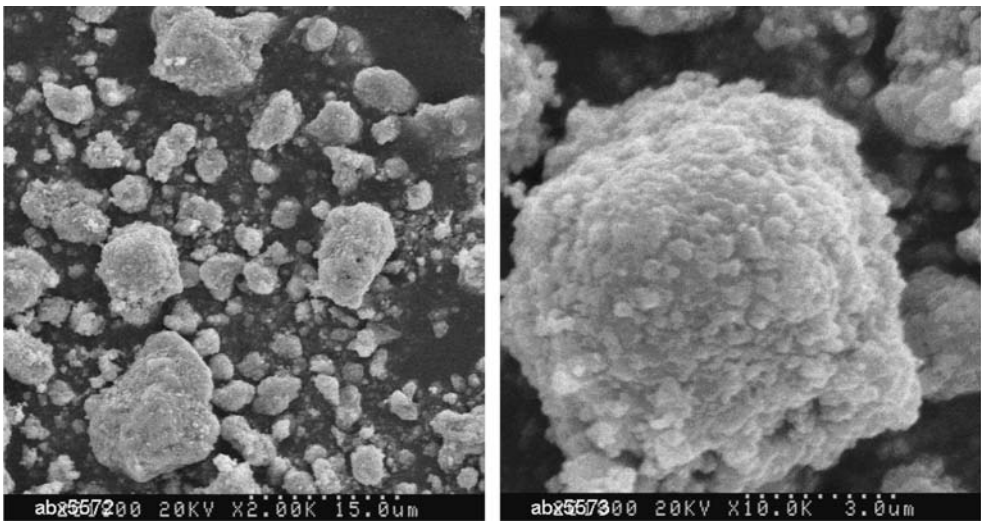


**Fig. 3** SEM photographs for $LiNi_{0.65}Co_{0.20}Mn_{0.15}O_2$ compound

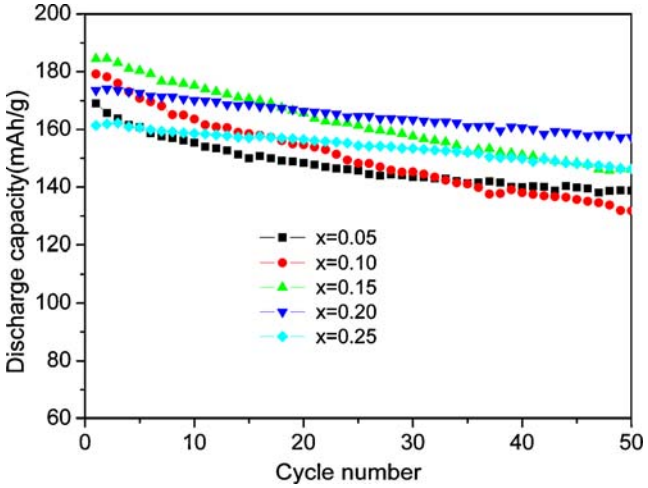


**Fig. 5** Discharge capacity as functions of cycle number for $LiNi_{0.85-x}Co_xMn_{0.15}O_2$ in the voltage range 3.0–4.3 V

distribution of cations in the layered structure and consequently restrain the possible degradation of structure in the process of charge and discharge [15], while too much Co doping would decrease the capacity. As to the $LiNi_{0.85-x}Co_xMn_{0.15}O_2$ series, the amount of Co doping at 0.20 has the best electrochemical performance. The initial discharge capacity of $LiNi_{0.65}Co_{0.20}Mn_{0.15}O_2$ is 173.6mAh $g^{-1}$, and the capacity rention after 50 cycles is still 90.6%. Our method can decrease the calcining temperature compared to the solid-state reaction [30] and coprecipitation method [31], and the materials prepared by our method have better electrochemical properties.

Figure 6 shows the charge–discharge curves of the first and 20th cycle for $LiNi_{0.65}Co_{0.20}Mn_{0.15}O_2$ in different voltage ranges. The initial discharge efficiency in different voltage ranges are all comparatively high, which indicates that the 3a sites of the material are in good order for $Li^+$ intercalation/deintercalation [32]. When the voltage range becomes wider, the cyclic performance decreases. Venkatraman et al. [33] reported that oxygen loss from layered metal oxide cathodes became significant above 4.25V vs Li. This may lead to the cycling losses, unless steps are taken to reduce oxygen activity. It can adopt the surface coating with metal oxides, such as $ZrO_2$, $Al_2O_3$, and $TiO_2$ [34–36], which may bond to surface oxygen and reduce oxygen activity.

A DSC study of the $LiNi_{0.65}Co_{0.20}Mn_{0.15}O_2$ electrode was carried out after charging the cell to 4.3V at 50mA $g^{-1}$. As shown in Fig. 7, the electrode material has an exothermic peak at 274 °C, and the $\Delta H$ is 21.73 J $g^{-1}$. The exothermic peak shifts to a higher temperature implying improved safety, compared to 230 °C for the $LiCoO_2$ material [37].

## Conclusions

$LiNi_{0.85-x}Co_xMn_{0.15}O_2$ cathode materials were synthesized by a rheological phase reaction method. Reactants are homogeneously mixed at atomic scale by our method, which decreases the sintering time and temperature remarkably. The products all have high reversible capacity and good cyclic performance. The initial charge and discharge capacity of $LiNi_{0.65}Co_{0.20}Mn_{0.15}O_2$ was 197.8 and 173.6 mAh $g^{-1}$, respectively. The capacity rention after 50 cycles is still 90.6%. The excellent electrochemical properties indicated that the best content of Co is 0.20 as to the $LiNi_{0.85-x}Co_xMn_{0.15}O_2$ series. Therefore, our method is a simple and effective method to prepare cathode materials for lithium-ion batteries.

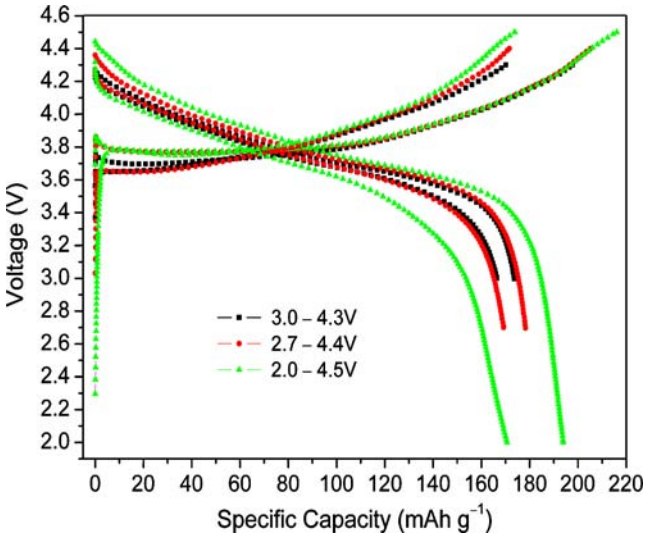


**Fig. 6** Charge–discharge curves of the first and 20th cycle for $LiNi_{0.65}Co_{0.20}Mn_{0.15}O_2$ in the different voltage ranges

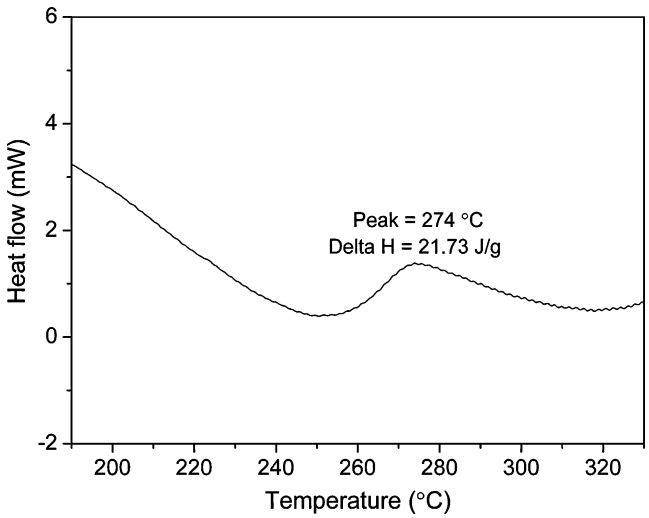


**Fig. 7** DSC curve of $LiNi_{0.65}Co_{0.20}Mn_{0.15}O_2$ electrode charged to 4.3 V

**Acknowledgments** We gratefully acknowledge the financial support from the National Nature Science Foundation of China (no. 29833090 and no. 29771025).

## References

1. Nagaura T, Tozawa K (1990) Prog Batteries Sol Cells 9:209
2. Koksbang R, Barker J, Shi H, Saidi MY (1996) Solid State Ion 84:1
3. Ohzuku T, Ueda A (1994) J Electrochem Soc 141:2972
4. Davidson I, Greedan JE, von Sacken U, Michal CA, Dahn JR (1991) Solid State Ion 46:243
5. Kweon HJ, Kim GB, Lim HS, Nam SS, Park DG (1999) J Power Sources 83:84
6. Kang SH, Kim J, Stoll ME, Abraham D, Sun YK, Amine K (2002) J Power Sources 112:41
7. Fey GTK, Subramanian SV, Chen JG, Chen CL (2002) J Power Sources 103:265
8. Oh SH, Jeong WT, Cho WI, Cho BW, Woo K (2005) J Power Sources 140:145
9. Huang YQ, Guo WY, Li DC, Peng ZH, Zhou YH (2005) Chin J Inorg Chem 21:736
10. Amatucci GG, Tarascon JM, Klein LC (1996) J Electrochem Soc 143:1114
11. Arora P, White RE, Doyle M (1998) J Electrochem Soc 145:3647
12. Ohzuku T, Makimura Y (2001) Chem Lett 7:642
13. Patoux S, Doeff MM (2004) Electrochem Commun 6:767
14. Myung ST, Lee MH, Komaba S, Kumagai N, Sun YK (2005) Electrochim Acta 50:4800
15. Yoshio M, Noguchi H, Itoh JI, Okada M, Mouri T (2000) J Power Sources 90:176
16. Li DC, Noguchi H, Yoshio M (2004) Electrochim Acta 50:427
17. Choi J, Manthiram A (2005) Solid State Ion 176:2251
18. Choi J, Manthiram A (2006) J Power Sources 162:667
19. Liang YG, Yang SJ, Yi ZH, Sun JT, Zhou YH (2005) J Mater Sci 40:5553
20. Wang CW, Ma XL, Cheng JG, Zhou LQ, Sun JT, Zhou YH (2006) Solid State Ion 177:1027
21. Wang CW, Ma XL, Li ZC, Liang YG, Sun JT, Zhou YH (2006) Electrochem Commun 8:289
22. Cao XY, Zhan H, Xie JG, Zhou YH (2006) Mater Lett 60:435
23. Wang GX, Zhong S, Bradhurst DH, Dou SX, Liu HK (1998) J Power Sources 76:141
24. Cho J, Kim G, Lim HS (1999) J Electrochem Soc 146:3571
25. Kinoshita A, Yanagida K, Yanai A, Kida Y, Funahashi A, Nohma T, Yonezu I (2001) J Power Sources 102:283
26. Dahn JR, Sacken UV, Michel CA (1990) Solid State Ion 44:87
27. Gao Y, Yakovleva MV, Ebner WB (1998) Electrochem Solid-State Lett 1:117
28. Ohzuku T, Ueda A, Nagayama M, Iwakoshi Y, Komori H (1993) Electrochim Acta 38:1159
29. Kim HS, Kim Y, Kim S, Martin SW (2006) J Power Sources 161:623
30. Gan CL, Hu XH, Zhan H, Zhou YH (2005) Solid State Ion 176:687
31. Zhang Y, Cao H, Zhang J, Xia BJ (2006) Solid State Ion 177:3303
32. Gover RKB, Kanno R, Mitchell BJ, Yonemura M, Kawamoto Y (2000) J Electrochem Soc 147:4045
33. Venkatram S, Manthiram A (2003) Chem Mater 15:5003
34. Lee SM, Oh SH, Ahnc JP, Cho WIL, Jang H (2006) J Power Sources 159:1334
35. Kim Y, Kim HS, Martin SW (2006) Electrochim Acta 52:1316
36. Li D, Kato Y, Kobayakawa K, Noguchi H, Sato Y (2006) J Power Sources 160:1342
37. Baba Y, Okada S, Yamaki JI (2002) Solid State Ion 148:311